Vol. 2, No. 1, pp. 12-16, June 2003

INTERNATIONAL JOURNAL OF SAFETY
www.kiis.or.kr

A Numerical Study on Methane-Air Counterflow Diffusion Flames Part 2. Global Strain Rate

Woe Chul Park*

Department of Safety Engineering, Pukyong National University, Busan 608-739, Korea

(Received March 27, 2003; Accepted May 30, 2003)

Abstract : In Part 1, the flame structure of the counterflow nonpremixed flames computed by using Fire Dynamics Simulator was compared with that of OPPDIF for different concentrations of methane in the fuel stream. In this study, comparisons were made for the global strain rate that is an important parameter for diffusion flames for further evaluation of FDS. At each of the three fuel concentrations, 20% CH_4 + 80% N_2, 50% CH_4 + 50% N_2, 90% CH_4 + 10% N_2 in the fuel stream, the temperature and axial velocity profiles were investigated for the global strain rate in the range from 20 to 100 s^{-1}. Changes in flame thickness and radius were also compared with OPPDIF. There was good agreement in the temperature and axial velocity profiles between the axisymmetric simulations and the one-dimensional computations except for the regions where the flame temperature reach its peak and the axial velocity rapidly changes. The simulations of the axisymmetric flames with FDS showed that the flame thickness decreases and the flame radius increases with increasing global strain rate.

Key words : counterflow flame, methane, global strain rate, flame thickness, flame radius

1. Introduction

With development of high performance computers and computational fluid dynamics (CFD), large scale fire simulations are available on a PC in three-dimensional unsteady situations. One of such fire codes is the Fire Dynamics Simulator (FDS) [1], developed by the National Institute of Standards and Technology (NIST). FDS adopted two different methods in computing the turbulent flow fields: large eddy simulations (LES) and direct numerical simulations (DNS).

Since DNS is more suitable for simulations of the diffusion flames computing directly transport and dissipative process, it have been applied to the axisymmetric counterflow flames as mentioned in Part 1. For an evaluation of FDS, in Part 1, the flame structure was compared between FDS and OPPDIF [2], which is a one-dimensional flame code, in a wide range of methane concentrations from 20% to 100% by volume in the fuel stream. In Part 2, further investigations were made for the global strain rate. The objective of this study is to investigate for various global strain rates to see whether the results of FDS which employed a mixture fraction formulation agree with those of OPPDIF which includes detail chemistry. The effects of global strain rate on the flame thickness and radius were also investigated.

2. Methodology

The same counterflow burner as Part 2 shown in Fig. 1 was used. There are two opposed circular ducts, the diameter of 15 mm and the wall thickness of 0.5 mm, separated by a distance of 15 mm. A mixture of fuel and

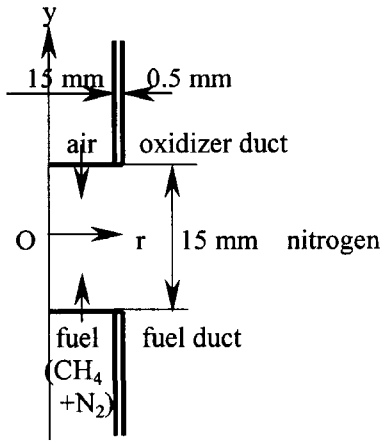

Fig. 1. Schematic of the counterflow burner.

*Corresponding author: wcpark@pknu.ac.kr

agent(nitrogen) flows in the lower fuel duct, and air flows in the upper oxidizer duct. Combustion takes place in quiescent nitrogen gas. The oxidizer is pure air and the fuel is composed of a mixture of methane and nitrogen.

The global strain rate, a_g is defined as

$$a_g = \frac{2V_A}{L}\left[1 + \frac{V_F}{V_A}\left(\frac{\rho_F}{\rho_A}\right)^{0.5}\right] \quad (1)$$

where V_A is the velocity of the oxidizer stream (air) and V_F is that of the fuel stream (mixture of methane and nitrogen) at the duct exits. L is the separation distance between the two ducts (15 mm), ρ_A is the density of air, and ρ_F is the density of fuel. For the given global strain rates, V_A and V_F are the same and calculated from the above definition.

The top hat velocity profile was imposed at the both duct exits, no slip condition on the duct walls, and T = 25°C in the fuel and air streams. FDS employed a mixture fraction formulation as combustion model. The solution procedures are described in detail in McGrattan *et al.* [1] and Park and Hamines [3].

The computational domain was taken to be 40 mm×40 mm, and 80×80 uniform grids. The average temperature and axial velocity along the center line (y axis) were calculated from the instantaneous values of 0.8~1.0 s.

3. Results and Discussion

3-1. Temperature and Axial Velocity

When the fuel is composed of 20% methane and 80% nitrogen, the temperature and axial velocity profiles along the duct centerline (y axis) of FDS and OPPDIF

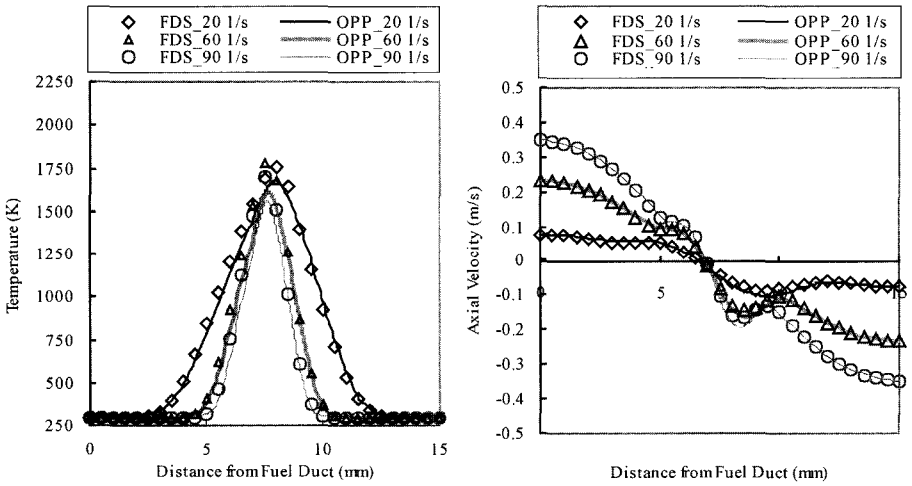

(a) temperature (b) axial velocity

Fig. 2. Comparison of temperature and axial velocity profiles for global strain rates (fuel of 20%CH_4 + 80%N_2).

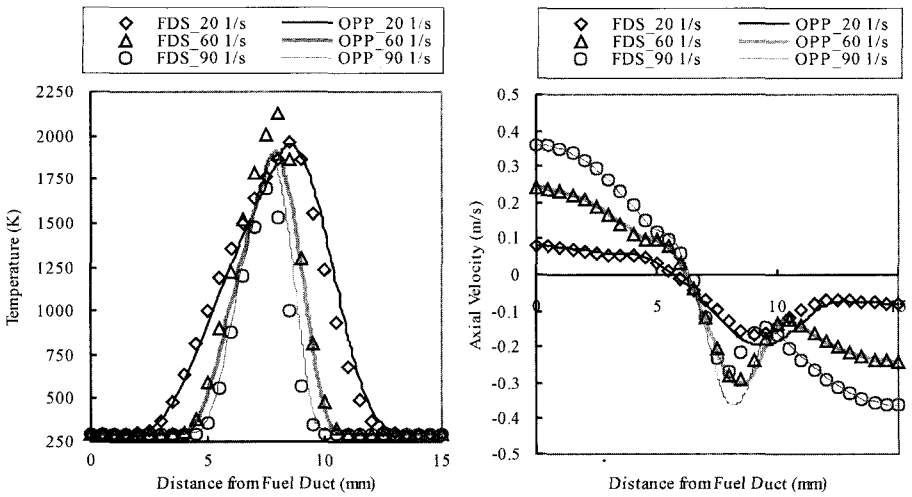

(a) temperature (b) axial velocity

Fig. 3. Comparison of temperature and axial velocity profiles for global strain rates (fuel of 50%CH_4 + 50%N_2).

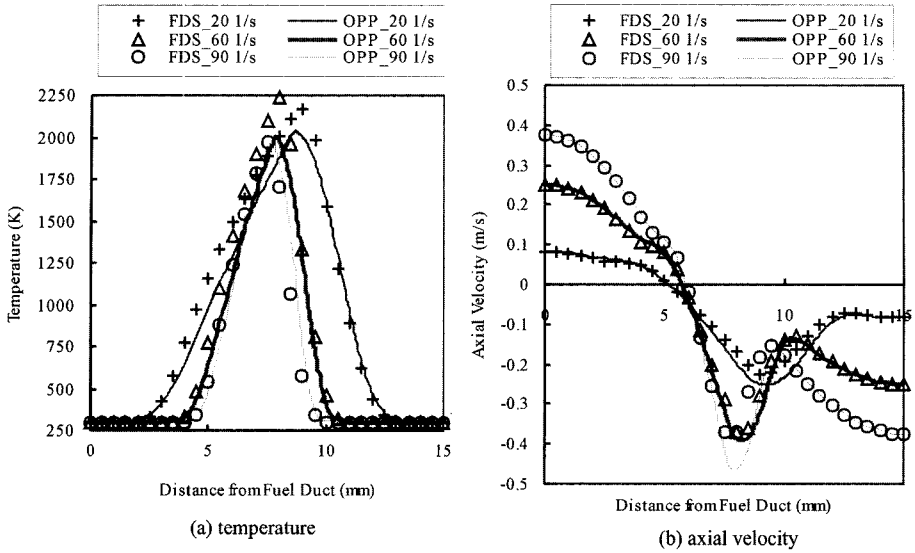

Fig. 4. Comparison of temperature and axial velocity profiles for global strain rates (fuel of 90%CH_4 + 10%N_2).

are compared in Fig. 2 for different global strain rates, $a_g = 20$, 60 and 90 s^{-1}. The temperature and velocity profiles for the global strain rates are in excellent agreement in this near-extinction fuel concentration case.

Fig. 3 compares the temperature and axial velocity profiles of FDS and OPPDIF for the three global strain rates, $a_g = 20$, 60 and 90 s^{-1} when the fuel is a mixture of 50% methane and 50% nitrogen. It shows that there is some discrepancy in the peak flame temperature, and the velocity near the flame for $a_g = 90$ s^{-1}. Except that the results of FDS agree well with those of OPPDIF. The flame is positioned nearly at the center between the two ducts (distance of 7.5 mm from the fuel duct) at the moderate strain rates, $a_g = 60$ and 90 s^{-1}, whereas its position is shifted towards the upper oxidizer duct and the flame is much thicker at the low strain rate, $a_g = 20$ s^{-1} compared to the moderate strain rates. FDS predicts accurately and the change in the flame position and thickness.

Fig. 4 also compares the temperature and axial velocity profiles for different global strain rates in the case of the fuel of 90% methane and 10% nitrogen. Although there are small differences in the peak flame temperature and the velocity near the flame, the temperature and axial velocity profiles of the two numerical method are in good agreement. This fuel concentration also shows that prediction of FDS in the flame thickness and shift of the flame positions due to the global strain rate is accurate.

For the three different fuel concentrations the results of the axisymmetric counterflow flames by using FDS agrees very well with those of OPPDIF. It is very interesting that FDS, a three-dimensional fire simulation code with a mixture fraction combustion which does not include any detail chemistry, well predicts the flame structure.

3-2. Flame Radius and Thickness

Comparisons between FDS and OPPDIF over a wide range of fuel concentrations and global strain rates in Part 1 and Section 3.1 showed very good results of FDS for the counterflow diffusion flames in zero grav-

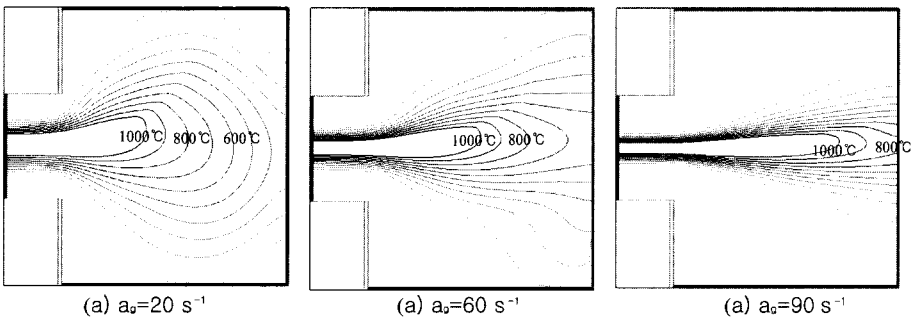

Fig. 5. Isotherms of 20%CH_4 + 80%N_2 for different global strain rates (FDS).

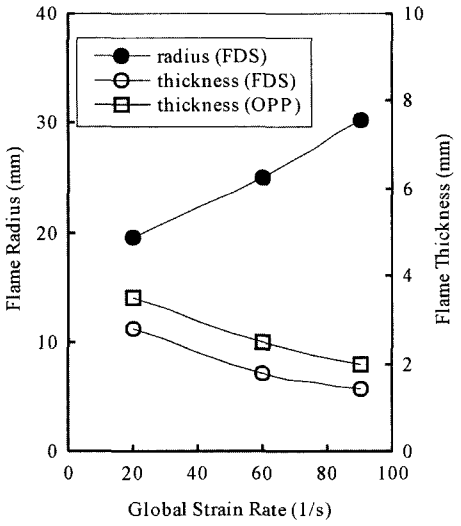

Fig. 6. Flame radius and thickness vs. global strain rate for fuel of 20% CH_4 + 80% N_2.

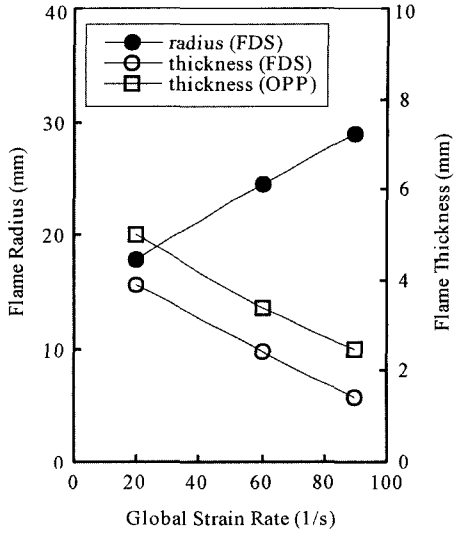

Fig. 8. Flame radius and thickness vs. global strain rate for fuel of 50% CH_4 + 50% N_2.

ity conditions. Further investigations were made for the effects of the global strain rate on the flame radius and thickness. The flame radius and thickness computed by FDS were measured from the isotherm of 1000°C, and the flame thickness of OPPDIF was measured from the temperature profile shown in Fig. 2~4. No results on the flame radius of OPPDIF are available since OPPDIF is a one-dimensional flame code.

In Fig. 5, the flames for the fuel of 20% CH_4 and 80% N_2 were compared with isotherms for $a_g = 20$, 60 and 90 s^{-1}. The isotherms represent the flame temperature from 0°C to 1000°C increasing by 100°C. As the global strain rate increases from $a_g = 20$ to 60 and 90 s^{-1}, stretch of the flame is increased.

Fig. 6 depicts the flame radius and thickness based on T = 1000°C. The flame radius, measured from the isotherm of 1000°C, increases with the global strain rate almost linearly. Eq. 1 shows that the axial velocity in the fuel and oxidizer streams is proportional to the global strain rate, and this results in the increase of the flame radius. The flame thickness at the duct center decreases with the increasing global strain rate while the flame is stretched. Both FDS and OPPDIF show a similar decreasing rate of the flame thickness with increasing global strain rate.

The isotherms for the three global strain rates for the fuel of 50% CH_4 + 50% N_2 are compared in Fig. 7. Each isotherm stands for 100°C increment. It is clearly shown that the flame becomes thinner and its radius increases with the global strain rate.

The flame radius and thickness versus the global strain rate in this case is plotted in Fig. 8. Increase in the flame radius and decrease in the flame thickness with the increasing global strain rate are similar to the case of fuel of 50% CH_4 + 50% N_2.

Figs. 9 and 10 respectively depict the isotherms of the flame and flame radius and thickness for the fuel of 90% CH_4 + 100% N_2. The results are very similar to those shown for the fuels of 20% CH_4 + 50% N_2 and 90% CH_4 + 100% N_2.

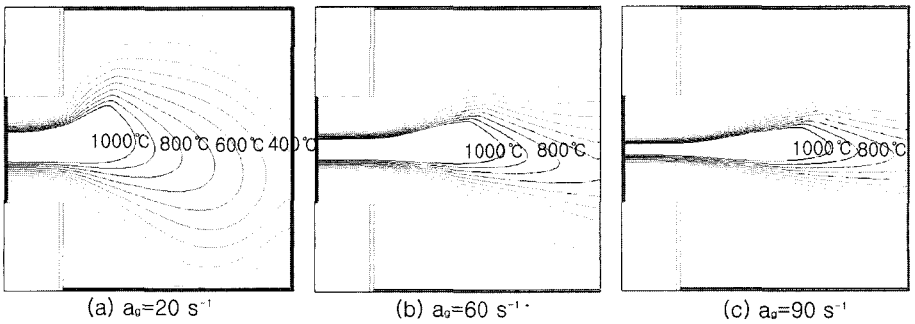

Fig. 7. Isotherms of 50% CH_4 + 50% N_2 for different global strain rates (FDS).

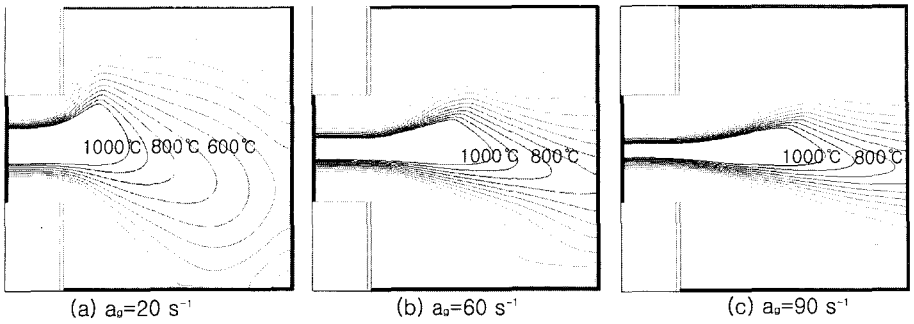

Fig. 9. Isotherms of 90% CH_4 + 10% N_2 for different global strain rates (FDS).

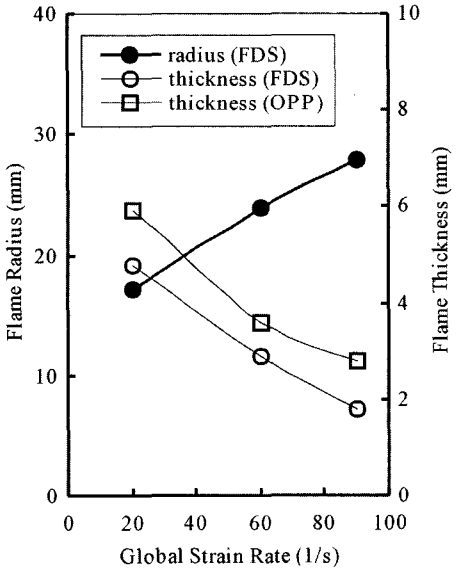

Fig. 10. Flame radius and thickness vs. global strain rate for fuel of 90% CH_4+ 10% N_2.

The flame radius shown in above comparisons showed nearly linear increase of the flame radius and with the global strain rate regardless of the fuel concentration, while the flame thickness decreases. The flame thickness predicted by FDS was smaller than that of OPPDIF, the decreasing rate of the flame thickness with increasing global strain rate obtained from the isotherms of FDS was, however, consistent with OPPDIF for all the three fuel concentrations.

4. Conclusions

The structure of counterflow flames for the global strain rate was compared between FDS and OPPDIF for further evaluation of FDS. The temperature and axial velocity profiles were compared for the global strain rates in the range from 20 to 100 s^{-1} at each of three methane concentrations, 20%, 50% and 90% by volume in the fuel stream. FDS predicted well the temperature and axial velocity profiles except for the regions of the peak flame temperature. The results of FDS showed almost linear increases in the flame radius and decrease in the flame thickness with increasing global strain rate. The trend of decreasing rate in the flame thickness of FDS was consistent with that of OPPDIF, though FDS over-predicted the flame thickness, regardless of the fuel concentrations.

Acknowledgement

This work was supported by Pukyong National University Research Fund in 2002.

References

[1] K. B. McGrattan, H. R. Baum, R. G. Rehm, A. Hamins, G. P. Forney, J. E. Floyd and S. Hostikka, "Fire Dynamics Simulator Technical Reference Guide", v.3, National Institute of Standards and Technology, Gaithersburg, MD, U.S.A, 2002.

[2] A. Lutz, R. J. Kee, J. Grcar and F. M. Rupley, "A Fortran Program Computing Opposed Flow Diffusion Flames", SAND96-8243, Sandia National Laboratories, Livermore, CA, U.S.A., 1997.

[3] W. C. Park and A. Hamins, "Development of a Three-Dimensional DNS Code for Study of Clean Agents - Two-Dimensional Simulation of Diluted Nonpremixed Counterflow Flames -", Intl J. of Safety, Vol. 1, No. 1, pp. 18~23, 2002.

Vol. 2, No. 1, pp. 17-22, June 2003

INTERNATIONAL JOURNAL OF SAFETY
www.kiis.or.kr

Analysis of Three Dimensional Crack Growth by Using the Symmetric Galerkin Boundary Element Method

Tae Soon Kim and Jai Hak Park[1]*

Nuclear Laboratory, Korea Electric Power Research Institute, Taejon, 305-380, Korea
*[1]*Department of Safety Engineering, Chungbuk National University, Cheongju, 361-763, Korea*

(Received April 7, 2003; Accepted June 3, 2003)

Abstract : In order to analyze general three dimensional cracks in an infinite body, the symmetric Galerkin boundary element method formulated by Li and Mear is used. A crack is modelled as distribution of displacement discontinuities, and the governing equation is formulated as singularity-reduced integral equations. With the proposed method several example problems for three dimensional cracks in an infinite solid, as well as their growth under fatigue, are solved and the accuracy and efficiency of the method are demonstrated.

Key words : galerkin method, stress intensity factor, three dimensional crack, boundary element method

1. Introduction

In structural integrity assessment and damage tolerance analysis, the calculation of fracture mechanics parameters for arbitrary three-dimensional surface and internal cracks remains an important task [1]. For this purpose, the finite element method (FEM) and the boundary element method (BEM) were combined satisfactorily.

The analysis of fracture mechanics by using the finite element methods for are well established. In addition, the use of energetic methods and in particular the equivalent domain integral method allows to obtain fracture mechanics parameters with acceptable accuracy [2, 3]. The finite element method to the analysis of three-dimensional cracks, however, is needed a lot of times and high costs in the mesh generation.

In the BEM for linear fracture mechanics problems, the mesh should be generated only for the boundary of the structure, and for the crack surface. Consequently, it is simpler to create a boundary element mesh, in comparison to a finite element mesh for a body with a crack. However, for a surface crack it is necessary to maintain mesh compatibility between the mesh on the crack surface, and that on the boundary of the structure. If it is necessary to analyze cracks of different sizes, both the crack-surface mesh and the mesh for the surface of the structure, should be modified. The traditional BEM has certain features, which makes it suitable for the solution of crack problems.

For the solution of two- and three-dimensional fracture mechanics problems, Keat, Annigeri and Cleary tried to combine the traditional hyper singular BEM and the FEM [4]. Based on the superposition principle the authors employ direct method for creating an equation system for the fracture mechanics problem. An obvious disadvantage of this approach is the large size of matrices responsible for interaction between finite element and boundary element global matrices and consequently large solution time.

The symmetric Galerkin boundary element method (SGBEM) is a way of satisfying the boundary integral equations of elasticity in a Galerkin weak form [5]. This method helps to overcome some drawbacks of the traditional boundary element approach. The SGBEM is characterized by weakly singular kernels. After a special transformation, which removes the singularity from kernels, the boundary element matrices can be integrated with the use of usual Gaussian rule.

In this paper, the symmetric Galerkin boundary element method for the analysis of three dimensional cracks in infinite bodies is presented. The crack is modeled as a distribution of displacement discontinuities. The crack surface is discretized by quadratic eight-

*Corresponding author: jhpark@cbucc.chungbuk.ac.kr